

## CHANGE OF STRUCTURE OF THE CHERENKOV EMISSION AT MODULATED SOURCE IN DISPERSIVE METAMATERIALS

Gennadiy Burlak\* and Erika Martínez-Sánchez

Centro de Investigación en Ingeniería y Ciencias Aplicadas, Universidad Autónoma del Estado de Morelos, Cuernavaca, Mor., México

**Abstract**—We systematically study the Cherenkov optical emission by a nonrelativistic modulated source crossing 3D dispersive metamaterial. It is found that the interference of the field produced by the modulated source with the periodic plasmonic-polariton excitations in a metamaterial leads to the specific interaction in the frequency range where the dispersive refractive index of a metamaterial is negative and the reversed Cherenkov emission is generated. Such resonance considerably modifies the spatial structure of the Cherenkov field. In our study parameters of a metamaterial and modulated source are fixed while the frequency spectrum of the plasmonic excitations is formed due to the fields interplay in the frequency domain.

### 1. INTRODUCTION

Nanophotonics is the study of the behavior of light on the nanometer scale with involving the interaction of light with nano-structures. Novel optical properties of materials results from their extremely small size that have a variety of applications in nanophotonics and plasmonics. The investigations of optical negative-index [1] metamaterials (NIM) using the nanostructured metal–dielectric composites already have led to both fundamental and applied achievements that have been realized in various structures [2–26]. The main applications of negative index metamaterials (or left-handed materials (LHM)) are connected with a remarkable property: the direction of the energy flow and the direction of the phase velocity are opposite in NIM that results unusual properties of electromagnetic waves propagating in these mediums.

Cherenkov radiation by a charged source that moves in a left-handed material and has not the own frequency has been studied

---

*Received 20 March 2013, Accepted 20 April 2013, Scheduled 28 April 2013*

\* Corresponding author: Gennadiy Burlak (gburlak@uaem.mx).

in number of works [17–23]. Both experimental and theoretical frameworks are investigated, see review [18] and references therein. However, in some important cases a moving particle has the internal own frequency [27]  $\omega_0$ , for instance the ion oscillating at the transition frequency  $\omega_0$ . The Cherenkov emission in metamaterials for such situation is insufficiently investigated yet, although it is a logical extension of other works in this area.

In this paper, the Cherenkov optical radiation in 3D metamaterials by a nonrelativistic modulated source having the own frequency  $\omega_0$  with an emphasis on the dispersive properties of the medium is numerically studied. We performed the FDTD simulations with the use of the material parameters at various modulating frequencies  $\omega_0$ , however, without references to the operational frequency range.

## 2. BASIC EQUATIONS

In metamaterials, it is necessary to treat electromagnetic wave interactions with a metal ingredient using a dispersive formulation that allows correct description of the internal electron dynamics. It is well-known that realistic LHM (where for a range of frequency the negative refraction index  $n$  is expected) can be characterized by either Lorentz or Drude dispersion models, see, e.g., Ref. [25], Chapters 5, 6 and references therein. In case of a small collision frequency the study of nonlinear dynamical excitations is allowed [26]. In our paper, the opposite case is considered when the low frequency edge of magnetic forbidden band [25]  $\omega_{m0}$  is small enough with respect to the magnetic collision frequency  $\gamma_m \gg \omega_{m0}$ . The latter allows reducing the Lorenz model to the Drude model that is widely used for modeling in complex materials. The Maxwell equations read

$$\nabla \times \mathbf{E} = -\mu_0\mu_h \frac{\partial \mathbf{H}}{\partial t} - \mathbf{J}_m - \sigma_m \mathbf{H}, \quad (1)$$

$$\nabla \times \mathbf{H} = \varepsilon_0\varepsilon_h \frac{\partial \mathbf{E}}{\partial t} + q\mathbf{v}_0 f(r, t) \cos(\omega_0 t) + \mathbf{J}_e + \sigma_e \mathbf{E}, \quad (2)$$

where a radiating particle (bunch) has modulating frequency  $\omega_0$ ,  $\mathbf{J}_e$  is the electrical current and  $\mathbf{J}_m$  is the magnetic current which obey the following material equations

$$\dot{\mathbf{J}}_e + \gamma_e \mathbf{J}_e = b_e \mathbf{E}, \quad \dot{\mathbf{J}}_m + \gamma_m \mathbf{J}_m = b_m \mathbf{H}, \quad (3)$$

here  $\gamma_e$  and  $\gamma_m$  are the electrical and magnetic collision frequencies respectively,  $b_e = \varepsilon_0\omega_{pe}^2$ ;  $b_m = \mu_0\omega_{pm}^2$ ,  $\omega_{pe}$  and  $\omega_{pm}$  are frequencies of electric and magnetic plasmons respectively;  $\sigma_e$  and  $\sigma_m$  are conductivities;  $\varepsilon_h, \mu_h$  are dielectric and magnetic functions of the host

medium respectively [28, 29]. For metals such as silver, gold, copper and aluminum the density of the free electrons is on the order of  $10^{23} \text{ cm}^{-3}$ . The typical value  $\omega_{pe} \approx 2 \cdot 10^{16} \text{ s}^{-1}$  ([30], p.44). In a metamaterial with fishnet structure [14] we consider the charge particle (charge  $q$ ) moving with a uniform velocity parallel to  $x$  direction:  $\mathbf{v}_0 \parallel \hat{\mathbf{e}}_x$  and the density of the particle is defined by the Gaussian as  $f(r, t) = W^{-3} \exp\{ -[(x - v_0 t)^2 + y^2 + z^2]/W^2 \}$ , where  $W$  is the width; at  $W \rightarrow 0$  such a distribution is simplified to the isotropic point-source distribution  $f(r, t) \rightarrow (\pi)^{3/2} \delta(x - v_0 t) \delta(y) \delta(z)$ . In the following for simulations we use dimensionless variables, where for renormalization are used: the vacuum light velocity  $c = (\varepsilon_0 \mu_0)^{-0.5}$  and the typical spatial scale for nanooptics objects  $l_0 = 75 \text{ nm}$ . With such a normalization above indicated the metal plasma frequency becomes  $\omega_{pe} = 5$ . The electrical and magnetic fields are renormalized with the electrical scale  $E_0 = ql_0 \varepsilon_0$  and magnetic scale  $H_0 = (\varepsilon_0 / \mu_0)^{0.5} E_0$  respectively. Some metamaterials exhibit anisotropic properties with tensor permittivity and permeability. To seek for simplicity, in this paper, we concentrated in the isotropic geometry. Modeling anisotropic medium is a straightforward extension of this model, see details in [18, 23].

In our FDTD simulations (in time domain) we use the following idea. In optical experiments normally one refers only to the parameters of material ( $\gamma_e$ ,  $\sigma_e$ ,  $\omega_{pe}$ , and  $\gamma_m$ ,  $\sigma_m$ ,  $\omega_{pm}$ ). Therefore, we consider the Cherenkov emission produced by a particle with modulating frequency  $\omega_0$ , with the use only the material parameters and without of references to the operational frequency band. In this approach, the frequency spectrum of internal excitations  $\omega$  is left as a free parameter that is defined from simulations by a self-consistent way. For 3D dispersion material such a problem becomes too difficult for analytical consideration. In this paper, the well-known numerical algorithms in the time domain [31] were used, for details see Ref. [11].

General 3D case in Cartesian coordinates is considered since such a geometry normally is used on the optical investigations [14]. We examine a spatially averaged metamaterial composition: nanostructured metal-dielectric composites (fishnet), similarly that was used in the experiment [14]. In this case, the spatial average scale is less then the infrared and visual wavelengths, so we can deem that the material (dielectric and magnetic) dispersion is allowed by the Drude model and the role of the active dielectric ingredient is reduced to a compensation of losses due to the metal ingredient. In our simulations was used the numerical grid  $L^3$ ,  $L = 100, 120, 150$ , for more details see Ref. [11].

The following steps have been used in our approach: (i) First, we calculated the time-spatial field dynamics that is raised by the

crossing radiating particle for different modulating frequencies  $\omega_0$ , Eqs. (1)–(3). (ii) In second step we applied the Fourier analysis for the time and spatial dependencies of the field calculated in the first step in order to reveal the dynamics and spectrum of internal excitations. The following dimensionless parameters were used in our simulations:  $\omega_{pe} = 5$ ,  $\omega_{pm} = 7$ ,  $\varepsilon_h = 1.44$ ,  $\mu_h = 1$ ,  $\gamma_e = \gamma_m = 10^{-4}$ ,  $\sigma_e = \sigma_m = 10^{-7}$ ,  $W = 4$ ,  $q_2 = 2$ . We also varied the particle velocity  $v_0$  for different  $\omega_0$  to study regimes of the Cherenkov emission. Our results are shown in Figs. 1–5.

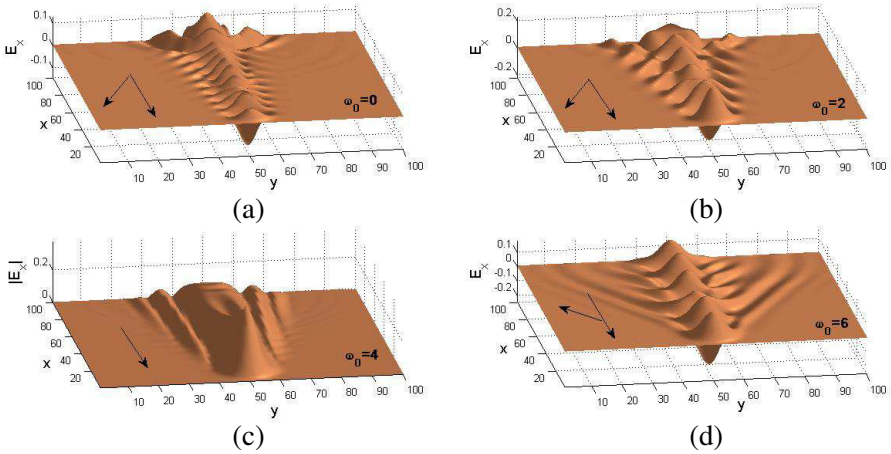


**Figure 1.** Snapshots of the Cherenkov field emission  $E_x(r, t)$  generated by radiating particle with velocity  $v_0 = 0.52$  for different frequencies  $\omega_0$  at time  $t \simeq 190$  in a dispersive metamaterial. (a)  $\omega_0 = 0$ ; in this case, the complementary Cherenkov angle is negative  $\theta_1 < 0$ ; (b)  $\omega_0 = 2.0$ ,  $\theta_1 < 0$ ; (c)  $\omega_0 = 4.0$ ,  $\theta_1 \simeq 0$ ; (d)  $\omega_0 = 6.0$ ; in this case, the angle is positive  $\theta_1 > 0$ . The oscillations in the top of the figures exhibit the shock waves arising by charged source at the beginning of motion (see [32], Chapter 2).

Figure 1 shows the spatial structure of  $E_x(r, t)$  field for the particle with modulating frequency  $\omega_0$  that moves with uniform velocity  $v_0 = 0.52$ . Fig. 1(a) depicts the case  $\omega_0 = 0$ ; in this situation only the spectrum of the periodic plasmonic excitations with the frequency  $\omega_C$  and negative phase velocity is observed (see details in Ref. [11]). At the increase of  $\omega_0$  up to 6 (see Figs. 1(b), (c) and (d) respectively) the spatial field structure changes considerably. For  $\omega_0 = 2$  and  $\omega_0 = 6$  (see Figs. 1(b) and (d) respectively) the field has oscillating shape, but

for  $\omega_0 = 4$  in Fig. 1(c) the field acquires a near monotonic form.

In what follows we use the complementary Cherenkov emission angle  $\theta_1 = \pi/2 - \theta$ , where [28]  $\cos(\theta) = c/nv_0$ . For such angle we have [11]  $\cos(\theta) = \sin(\theta_1) = c/nv_0$ , so for conventional material (with  $\text{Re}(n) > 0$ )  $\theta_1$  is positive  $\theta_1 = \theta_{1+} > 0$ , while for negative refraction index metamaterial NIM (with  $\text{Re}(n) < 0$ )  $\theta_1$  is negative  $\theta_1 = \theta_{1-} < 0$ . From Fig. 1 we observe that for frequencies  $\omega_0 \leq 3$  the angle  $\theta_1$  is negative what corresponds to the reverse Cherenkov radiation. But for larger  $\omega_0 \geq 6$  the Cherenkov radiation already acquires conventional structure with positive  $\theta_1 > 0$ , see Fig. 1(d). More interesting is found the intermediate case with  $\omega_0 \simeq 4$  where the field acquires nearly monotonic shape, see Fig. 1(c). Such a behavior can be interpreted as a transition in the spectra of plasmonic-polariton excitations. Further, we study such field behavior with details.

The interesting question emerges, why the structure of field in Fig. 1 changes so considerably with the change of the modulating frequency  $\omega_0$ ? To study that we explore the variation of the field spatial structure in the wavenumber domain ( $k$ ) at the change  $\omega_0$ . It is instructively to compare the field spatial structure with  $\omega_0 = 0$  in NIM with other modulated particle case when  $\omega_0 \neq 0$  but in a *dispersiveless* material (with  $\omega_{pe} = 0$ ,  $\omega_{pm} = 0$ ). (Such an evaluation in principle could be done similarly to the *Liènard-Wiechert potentials* approach [28], but analytical calculations of the field structure are difficult, so in this paper, we evaluate the field dependencies numerically in the framework of our model.) Such comparison is presented in Fig. 2 for the time  $t = t_0 \sim 190$  when the particle reaches the output side of the system. From Fig. 2 we observe that for dispersiveless and dispersive cases (left and right panels in Fig. 2 respectively) the fields  $E_x(x, t)$  have well-defined resonances in the wavenumber domain  $E_x(k, t)$  at  $k_s \simeq k_{s0} \simeq 4.33$  (resonance point). One can conclude that in this point a resonant interplay arises between the plasmonic-polariton spectrum and the modulating particle field. Corresponding changes are resonantly accumulated within the system length that finally leads to considerable modification of the field shape along the particle path.

Now we turn to other cases of the velocity  $v_0$  and modulation frequency  $\omega_0$ . To understand the effect deeper it is important to investigate the Doppler shift of the frequency  $\omega_0$  with respect of the rest metamaterial. For dispersiveless case ( $n = \text{const}$ ) the shifted frequency is calculated explicitly as  $\omega_{s0} = \omega_0/(1 + v_0n/c)$ . However, in dispersive case the shifted frequency  $\omega_{s0}$  acquires dependence on the dispersive refraction index of medium  $n(\omega)$ . For this situation, the shift already has to be evaluated from the complete equation

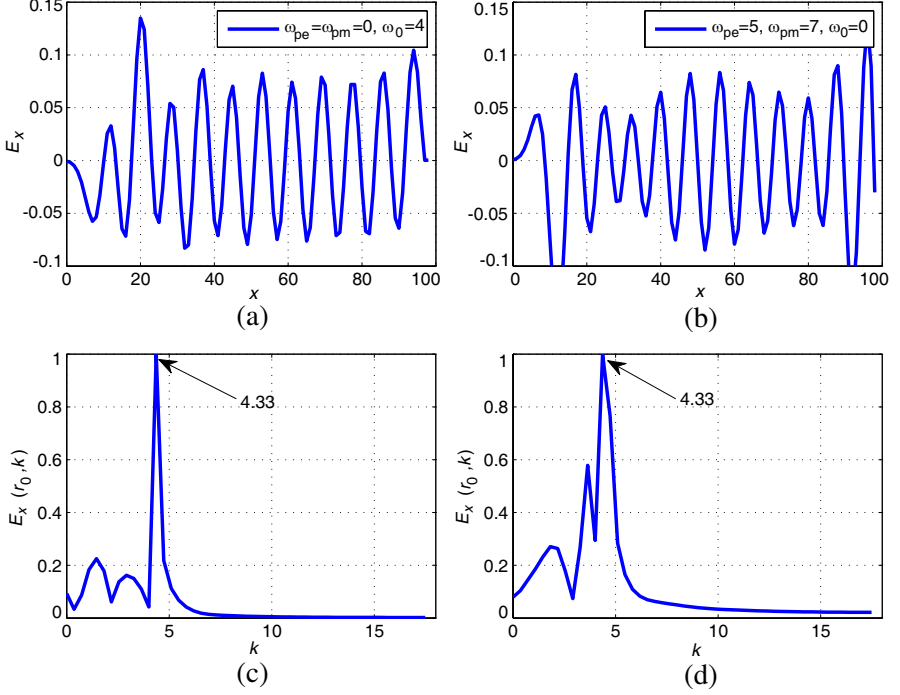


**Figure 2.** Field spatial structure  $E_x(x, t_0)$  in dispersiveless (left panels) and dispersive materials (right panels) accordingly for the time  $t = t_0 \simeq 190$  when the particle arrives the output of the system. (a) Field  $E_x(x, t_0)$  for dispersiveless case and  $\omega_0 = 4.0$ ; (b) spatial field in dispersive metamaterial but for  $\omega_0 = 0$ ; (c) Fourier spectrum (wavenumber domain)  $E_x(k, t_0)$  for (a) case; (d) Fourier spectrum  $E_x(k, t_0)$  for (b) case. We observe well-defined peaks  $k_s$  in both cases with  $k_s \simeq k_{s0} \simeq 4.33$ . See details in text.

$\omega_{s0} = \omega_0 / (1 + v_0 n(\omega_{s0}) / c)$ . The latter already requires the formulation of the dispersive material model for  $n(\omega)$ . But in used FDTD approach (the time domain) such the shift should be formed by a self-consistent way in NIM model, where in some frequency ranges the negativity of  $\text{Re}(n(\omega))$  can be reached. (In general the Doppler frequency shift has a nonlinear dependence on the modulating frequency, see details in Ref. [12].)

It is readily to see that  $k_s$  peak is calculated from the Doppler shift as  $k_s = \omega_{s0} n / c = \omega_0 n / c (1 + v_0 n / c)$ . To verify if the observed  $k_s$  is related to the Doppler shifted frequency  $\omega_0$  in Fig. 3 the dependence  $k_s = k_s(v_0)$  for various frequencies  $\omega_0$  in the dispersiveless case is

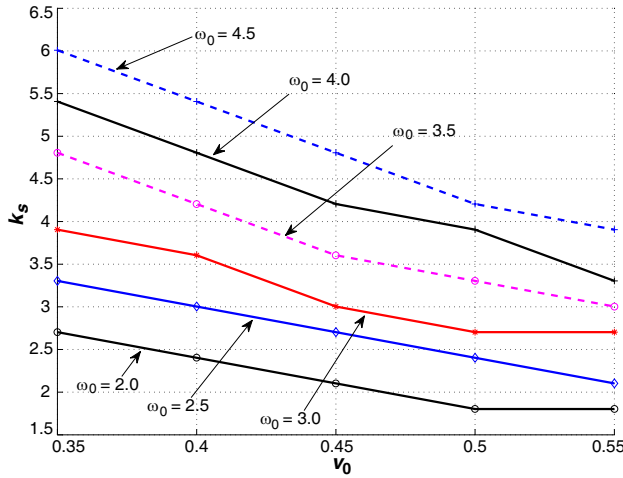


**Figure 3.** The dependence of the spectral peak position (wavenumber  $k_s$ ) of the field  $E_x(x, t)$  on the particle velocity  $v_0$  for different  $\omega_0$  at  $t \sim 190$  in dispersiveless case.

shown. From Fig. 3 we observe that (in used normalization) the wavenumber peak is about  $k_s \simeq 4.33$  for  $\omega_0 \simeq 4, v_0 = 0.52$  that coincides with peak  $k_{s0} = 4.33$  for no-modulated source at  $v_0 = 0.52$  for NIM in Fig. 1(a). Thus, we conclude that for  $\omega_0 \simeq 4$  and  $v_0 \simeq 0.52$  a spatial resonance arises due to Doppler effect around of  $|k_s - k_{s0}|$ .

Finally, we study the frequency spectra of the Cherenkov emission for different values of  $\omega_0$  and  $v_0$ . In the frequency domain the dispersive permittivity and permeability have the following form ([31] Chapter 9)  $\varepsilon(\omega) = \varepsilon_h - \omega_{pe}^2 / (\omega^2 + i\gamma_e\omega)$  and  $\mu(\omega) = \mu_h - \omega_{pm}^2 / (\omega^2 + i\gamma_m\omega)$ . For such  $\varepsilon(\omega)$  and  $\mu(\omega)$  the complex refractive index for the NIM metamaterial can be written as [33]

$$n(\omega) = \sqrt{|\varepsilon(\omega)\mu(\omega)|} e^{i[\phi_\varepsilon(\omega) + \phi_\mu(\omega)]/2}. \quad (4)$$

In this case, a peak frequency  $\omega = \omega_C$  has to be substituted into  $\varepsilon(\omega)$ ,  $\mu(\omega)$  and then in  $n(\omega)$  Eq. (4). Fig. 4 (left and right panels respectively) show the structure of field  $E_x(r, t)$  and the complex refractive indices  $n(\omega)$  in NIM for the cases different particle modulating frequencies  $\omega_0$  and velocity  $v_0 = 0.52$ . We observe from Fig. 4(a) that the field structures corresponds to the inverse Cherenkov emission. Fig. 4(c) shows that for  $\omega_0 = 2$  the plasmon-polaritons excitation (PPE) are generated at the peak frequency  $\omega_C = 3.77$  where the complex refractive index is  $n(\omega_C) = -0.87 - i8.10 \cdot 10^{-5}$ . For larger frequency  $\omega_0 = 3.9$  the field  $E_x$  has monotonic spatial structure, see

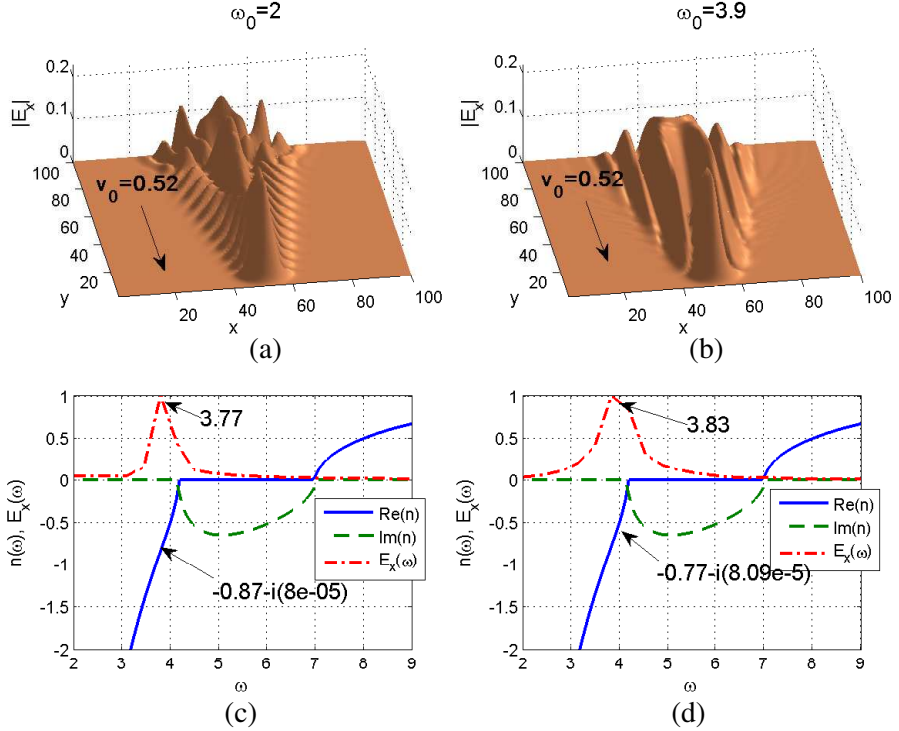


**Figure 4.** Snapshots of fields  $E_x(r, t)$  and the complex refractive indices  $n(\omega)$  in NIM for velocity  $v_0 = 0.52$  and different modulated frequencies  $\omega_0$ . (a) Field  $E_x$  for  $\omega_0 = 2$  corresponds to the plasmonic-polariton excitation (PPE) at the peak frequency  $\omega_C = 3.77$  where  $\text{Re}(n(\omega_C)) = -0.87$  indicated in (c); (b) field  $E_x$  for  $\omega_0 = 3.9$  that generate PPE at the peak frequency  $\omega_C = 3.83$  where  $\text{Re}(n) = -0.77$ .

Fig. 4(b) that allows exciting PPE at the peak frequency  $\omega_C = 3.83$  where  $n(\omega_C) = -0.77 - i8.09 \cdot 10^{-5}$ . In both cases,  $\text{Re}(n) < 0$ , thus, the optical waves have negative phase velocity that corresponds to reverse Cherenkov emission in NIM.

The situation for smaller  $v_0$  is shown in Fig. 5. Fig. 5 (left and right panels respectively) show the structure of field  $E_x(\mathbf{r}, t)$  and the complex refractive indices  $n(\omega)$  in NIM for the cases of particle with different modulating frequencies  $\omega_0$  and particle velocity  $v_0 = 0.35$ . We observe from Fig. 5(c) that for  $\omega_0 = 2$  the plasmon-polaritons excitation (PPE) are generated at the peak frequency  $\omega_C = 3.76$  where the complex refractive index is  $n = -0.89 - i8.0 \cdot 10^{-5}$ .



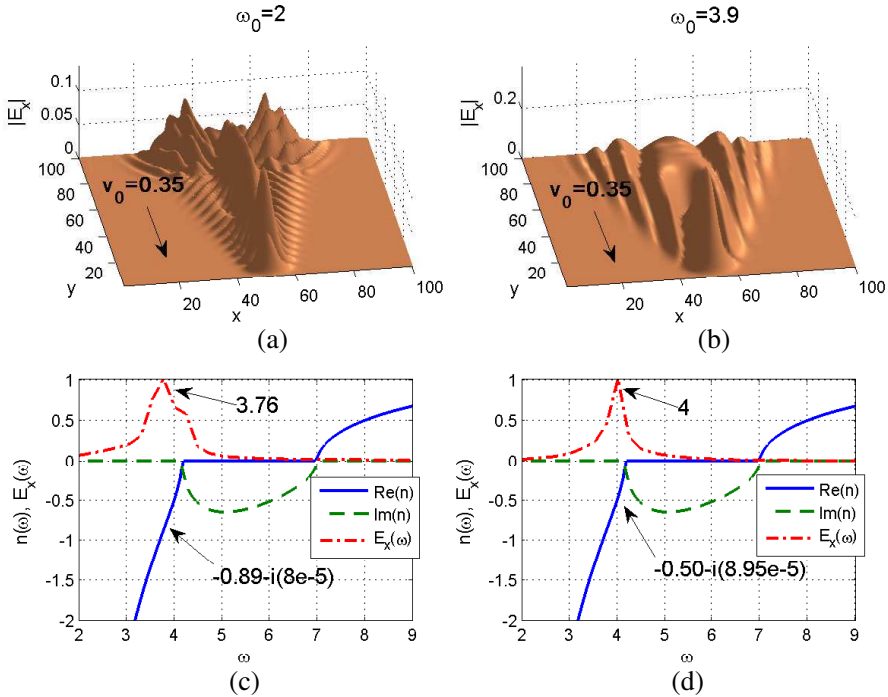


**Figure 5.** The same as in Fig. 4 but for velocity  $v_0 = 0.35$ . (a) Field  $E_x$  for  $\omega_0 = 2$  that generates the plasmon-polaritons excitation (PPE) at the peak frequency  $\omega_C = 3.76$  where  $\text{Re}(n) = -0.89$  (c); (b) field  $E_x$  for  $\omega_0 = 3.9$  that generate PPE at the peak frequency  $\omega_C = 4$  where  $\text{Re}(n) = -0.50$ .

Figures 4 and 5 show that the considered spatial resonance between the modulating frequency  $\omega_0$  and the plasmonic-polariton excitations: (i) happens in the frequency range where  $\text{Re}(n)$  is negative and the inverse Cherenkov emission occurs, and (ii) the value of the metamaterial refractive index (and thus the polariton phase velocity) depends on the particle velocity  $v_0$ . The latter in principle allows to control the property of PPE in metamaterial.

### 3. CONCLUSION

We numerically studied the Cherenkov optical emission by a nonrelativistic modulated source crossing 3D dispersive metamaterial. It is found that the resonant interaction of the field produced by

the modulated source with the spectrum of the periodic plasmonic-polariton excitations leads to considerable change of spatial structure for the Cherenkov emission. The field acquires monotonic shape in the frequency range where the dispersive refractive index of metamaterial is negative and the reversed Cherenkov radiation is generated. This effect opens new interesting possibilities in various applications metamaterials in nanophotonics with the potential for creating and control light confining structures to considerably enhance light-matter interactions.

## ACKNOWLEDGMENT

The work is partially supported by CONACyT grant 169496.

## REFERENCES

1. Veselago, V. G., "The electrodynamics of substances with simultaneously negative values of  $\varepsilon$  and  $\mu$ ," *Sov. Phys. Usp.*, Vol. 10, 509, 1968; *Usp. Fiz. Nauk*, Vol. 92, 517–526, 1967.
2. Shalaev, V. M., "Optical negative-index metamaterials," *Nature Photonics*, Vol. 1, 41–48, 2007.
3. Soukoulis, C. M. and M. Wegener, "Past achievements and future challenges in the development of three-dimensional photonic metamaterials," *Nature Photonics*, Vol. 5, 523–530, 2011.
4. Hess, O., J. B. Pendry, S. A. Maier, R. F. Oulton, J. M. Hamm, and K. L. Tsakmakidis, "Active nanoplasmonic metamaterials," *Nature Materials*, Vol. 11, 573–584, 2012.
5. Chen, H., C. T. Chan, and P. Sheng, "Transformation optics and metamaterials," *Nature Materials*, Vol. 9, 387–396, 2010.
6. Gordon, J. A. and R. W. Ziolkowski, "CNP optical metamaterials," *Opt. Express*, Vol. 16, 6692–6716, 2008.
7. Milton, G. W., "Realizability of metamaterials with prescribed electric permittivity and magnetic permeability tensors," *New Journal of Physics*, Vol. 12, 033035, 2010.
8. Podolskiy, V., A. Sarychev, and V. Shalaev, "Plasmon modes and negative refraction in metal nanowire composites," *Opt. Express*, Vol. 11, 735–745, 2003.
9. Shalaev, V. M., W. Cai, U. K. Chettiar, H.-K. Yuan, A. K. Sarychev, V. P. Drachev, and A. V. Kildishev, "Negative index of refraction in optical metamaterials," *Opt. Lett.*, Vol. 30, No. 24, 3356–3358, 2005.

10. Burlak, G., A. D-de-Anda, R. S. Salgado, and J. P. Ortega, "Narrow transmittance peaks in a multilayered microsphere with a quasiperiodic left-handed stack," *Optics Commun.*, Vol. 283, No. 19, 3569–3577, 2010.
11. Burlak, G., "Spectrum of Cherenkov radiation in dispersive metamaterials with negative refraction index," *Progress In Electromagnetics Research*, Vol. 132, 149–158, 2012.
12. Burlak, G. and V. Rabinovich, "Time-frequency integrals and the stationary phase method in problems of waves propagation from moving sources," *Symmetry, Integrability and Geometry: Methods and Applications*, Vol. 8, 096, 21, 2012.
13. Burlak, G. and A. D-de-Anda, "The field confinement, narrow transmission resonances and Green function of a multilayered microsphere with metamaterial defects," *Journal of Atomic, Molecular, and Optical Physics*, Article ID 217020, 1–13, 2011.
14. Xiao, S., V. P. Drachev, A. V. Kildishev, X. Ni, U. K. Chettiar, H.-K. Yuan, and V. M. Shalaev, "Loss-free and active optical negative-index metamaterials," *Nature*, Vol. 466, 735–738, 2010.
15. Deb, S. and S. D. Gupta, "Absorption and dispersion in metamaterials: Feasibility of device applications," *J. Phys.*, Vol. 75, No. 5, 837–854, 2010.
16. Cherenkov, P. A., "Visible emission of clean liquids by action of  $\gamma$ -radiation," *Dokl. Akad. Nauk.*, Vol. 2, 451–454, 1934.
17. Averkov, Y. O. and V. M. Yakovenko, "Cherenkov radiation by an electron particle that moves in a vacuum above a left-handed material," *Phys. Rev. B*, Vol. 79, 193402–193412, 2005.
18. Duan, Z. Y., B. I. Wu, S. Xi, H. S. Chen, and M. Chen, "Research progress in reversed Cherenkov radiation in double-negative metamaterials," *Progress In Electromagnetics Research*, Vol. 90, 75–87, 2009.
19. Xi, S., H. Chen, T. Jiang, L. Ran, J. Huangfu, B.-I. Wu, J. A. Kong, and M. Chen, "Experimental verification of reversed Cherenkov radiation in left-handed metamaterial," *Phys. Rev. Lett.*, Vol. 103, 194801, 2009.
20. Averkov, Y. O., A. V. Kats, and V. M. Yakovenko, "Electron beam excitation of left-handed surface electromagnetic waves at artificial interfaces," *Phys. Rev. B*, Vol. 72, 205110–205114, 2005.
21. Zhou, J., Z. Duan, Y. Zhang, M. Hu, W. Liu, P. Zhang, and S. Liu, "Numerical investigation of Cherenkov radiations emitted by an electron beam particle in isotropic double-negative metamaterials," *Nuclear Instruments and Methods in Physics*

- Research Section A*, Vol. 654, No. 1, 475–480, 2011.
22. Duan, Z. Y., Y. S. Wang, X. T. Mao, W. X. Wang, and M. Chen, “Experimental demonstration of double-negative metamaterials partially filled in a circular waveguide,” *Progress In Electromagnetics Research*, Vol. 121, 215–224, 2011.
  23. Duan, Z., C. Guo, and M. Chen, “Enhanced reversed Cherenkov radiation in a waveguide with double-negative metamaterials,” *Opt. Express*, Vol. 19, 13825–13830, 2011.
  24. Zhu, L., F.-Y. Meng, F. Zhang, J. Fu, Q. Wu, X. M. Ding, and J. L.-W. Li, “An ultra-low loss split ring resonator by suppressing the electric dipole moment approach,” *Progress In Electromagnetics Research*, Vol. 137, 239–254, 2013.
  25. Hao, Y. and R. Mittra, *FDTD Modeling of Metamaterials: Theory and Applications*, Artech House, 2009.
  26. Gabitov, I. R., R. A. Indik, N. A. Litchinitser, et al., “Double-resonant optical materials with embedded metal nanoparticles,” *J. Opt. Soc. Am. B*, Vol. 23, 535–542, 2006.
  27. Ginzburg, V. L., “Radiation by uniformly moving sources (Vavilov-Cherenkov effect, transition radiation, and other phenomena),” *Phys. Usp.*, Vol. 39, 973–982, 1996.
  28. Jackson, J. D., *Classical Electrodynamics*, John Wiley and Sons, 1975.
  29. Oughstun, K. E., *Electromagnetic and Optical Pulse Propagation 2: Temporal Pulse Dynamics in Dispersive, Attenuative Media* (Springer Series in Optical Sciences), Springer, 2009.
  30. Yeh, P., *Optical Waves in Layered Media*, John Wiley and Sons, New York, 1988.
  31. Taflov, A. and S. C. Hagness, *Computational Electrodynamics: The Finite-Difference Time-Domain Method*, Artech House, Boston, 2005.
  32. Afanasiev, G. N., *Cherenkov Radiation in a Dispersive Medium, Vavilov-Cherenkov and Synchrotron Radiation, Fundamental Theories of Physics*, Kluwer Academic Publishers, 2004.
  33. Ziolkowski, R. W., “Superluminal transmission of information through an electromagnetic metamaterial,” *Phys. Rev. E*, Vol. 63, 046604, 2001.